Deciphering the light vector meson contribution to the cross sections of e^+e^- annihilations into the open-strange channels through a combined analysis

Jun-Zhang Wang,[1,2,‡] Li-Ming Wang,[3,†] Xiang Liu,[1,2,4,*] and Takayuki Matsuki[5,§]

[1]*School of Physical Science and Technology, Lanzhou University, Lanzhou 730000, China*
[2]*Research Center for Hadron and CSR Physics, Lanzhou University and Institute of Modern Physics of CAS, Lanzhou 730000, China*
[3]*Key Laboratory for Microstructural Material Physics of Hebei Province, School of Science, Yanshan University, Qinhuangdao 066004, China*
[4]*Lanzhou Center for Theoretical Physics, Key Laboratory of Theoretical Physics of Gansu Province, and Frontiers Science Center for Rare Isotopes, Lanzhou University, Lanzhou 730000, China*
[5]*Tokyo Kasei University, 1-18-1 Kaga, Itabashi, Tokyo 173-8602, Japan*

(Received 29 June 2021; accepted 7 September 2021; published 28 September 2021)

In this work, we perform a combined analysis to the measured data of the cross section of open-strange processes $e^+e^- \to K^+K^-$, $e^+e^- \to K\bar{K}^* + \text{c.c.}$, $e^+e^- \to K^{*+}K^{*-}$, $e^+e^- \to K_1(1270)^+K^-$, $e^+e^- \to K_1(1400)^+K^-$, $e^+e^- \to K_2^*(1430)\bar{K} + \text{c.c.}$, and $e^+e^- \to K(1460)^+K^-$ with the support of study of hadron spectroscopy. We reveal the contribution of the possible light vector mesons around 2 GeV to reproduce the cross section data of the reported open-strange processes from e^+e^- annihilation which may provide a new perspective to construct the light vector meson family and understand the $Y(2175)$.

DOI: 10.1103/PhysRevD.104.054045

I. INTRODUCTION

Recently, the BESIII Collaboration released the data of the cross section for the open-strange process $e^+e^- \to K^+K^-$, where an obvious enhancement at 2.2 GeV was observed, and its Breit-Wigner resonance parameters were measured to be $M = 2239.2 \pm 7.1 \pm 11.3$ MeV and $\Gamma = 139.8 \pm 12.3 \pm 20.6$ MeV [1]. This is the first evidence showing the observation of the vector structure around 2.2 GeV in the open-strange channel. After that, BESIII reported the partial-wave analysis result of a new open-strange process $e^+e^- \to K^+K^-\pi^0\pi^0$, where the Born cross sections for the subprocesses $e^+e^- \to K^+(1460)K^-$, $K_1^+(1400)K^-$, $K_1^+(1270)K^-$, and $K^{*+}K^{*-}$ were measured [2]. By performing an overall fit to the above four processes, a structure with the mass of $2126.5 \pm 16.8 \pm 12.4$ MeV and the width of $106.9 \pm 32.1 \pm 28.1$ MeV was found, although a limited significance appears in the process $e^+e^- \to K_1^+(1270)K^-$ and $K^{*+}K^{*-}$ [2]. These new open-strange processes again indicate the existence of a vector structure around 2.2 GeV. When checking the data collected by the Particle Data Group (PDG) [3], one finds that the resonance parameter of this structure observed in these open-strange processes is close to the corresponding average value of that of the $Y(2175)$. Therefore, such simple comparison may suggest that this newly observed vector structure around 2.2 GeV and the $Y(2175)$ are the same state.

As we all know, the $Y(2175)$ was first reported in the process $e^+e^- \to \phi f_0(980)$ by the *BABAR* Collaboration based on the initial-state-radiation method [4], which was later confirmed in the same process by Belle [5] and in the process $J/\psi \to \eta\phi f_0(980)$ by BES [6] and BESIII [7]. Different from most of the observed charmoniumlike Y states, the $Y(2175)$ is the only light-flavor Y particle, which was reported in the hidden-strange final states and still remains a mystery even though more than a decade has passed since its discovery. Thus, it has inspired theorists great interests in exploring its inner structure. In the past years, the theoretical explanations for the $Y(2175)$ include hybrid $s\bar{s}g$ [8], vector strangeonium state $\phi(3S)$ [9,10], and $\phi(2D)$ [10–12], which should favor the open-strange decay modes. However, the recent BESIII measurements of the $e^+e^- \to K^+K^-$ [1] and $e^+e^- \to K^+K^-\pi^0\pi^0$ [2] reactions indicate that it is hard to understand these open-strange experimental data under the hybrid and strangeonium assignments to the $Y(2175)$. Interestingly, we notice that the experimental data of $e^+e^- \to K^+K^-\pi^0\pi^0$ was also

*Corresponding author.
xiangliu@lzu.edu.cn
†lmwang@ysu.edu.cn
‡wangjzh2012@lzu.edu.cn
§matsuki@tokyo-kasei.ac.jp

studied in a recent work [13,14], where $Y(2175)$ is considered to be a resonance structure from $\phi(1020)K\bar{K}$ dynamics, and $\pi^0\pi^0$ and K^+K^- come from the decay of $f_0(980)$ and the decay of $\phi(1020)$, respectively.

If the $Y(2175)$ is the $s\bar{s}g$ hybrid state, and the dominant decay modes should be $K_1(1270)^+K^-$ and $K_1(1400)^+K^-$ [8], while two open-strange decay channels like K^+K^- and $K^{*+}K^{*-}$ should be strongly suppressed according to the flux tube model analysis [15,16] and the QCD sum rule calculation [17,18]. On the other hand, different predictions for the branching ratios of the open-strange decay modes of strangeonium states $\phi(3S)$ and $\phi(2D)$ were given in former theoretical studies. For example, the branching ratio of $\phi(3S) \to K^+K^-$ was calculated to be almost zero in Ref. [9], and instead, $K_1(1270)^+K^-$ and $K^{*+}K^{*-}$ were predicted to be dominant decay channels of $\phi(3S)$ and $\phi(2D)$ in Refs. [9,10,12]. Furthermore, the theoretical total widths of $\phi(3S)$ and $\phi(2D)$ are generally estimated to be 200–400 MeV [9–12], which obviously deviates from the present experimental data of the $Y(2175)$ [3]. Therefore, the BESIII data [1,2] do not support the above theoretical predictions, which becomes a big challenge for the $s\bar{s}$ or $s\bar{s}g$ assignment to the $Y(2175)$. In addition to the above difficulties in decoding the $Y(2175)$ structure, there are still two confusing problems, which should be mentioned here. Through a comparison among the cross sections of the reported open-strange processes from e^+e^- annihilation, we can see that although the resonance parameter of the observed vector structure around 2.2 GeV in $e^+e^- \to K^+K^-$ [1] is similar to that in $e^+e^- \to K^+K^-\pi^0\pi^0$ [2], there is still about 100 MeV deviation on these measured masses. Hence, this measured mass discrepancy problem should be clarified. In addition, the BESIII measurement shows no observation of the structure around 2.2 GeV in a typical open-strange K^*K^* mode [2], which also should be appropriately understood.

When facing this puzzling situation, let us first return to the open-strange reaction itself, $e^+e^- \to K_{(J)}^{(*/\prime)}\bar{K}_{(J)}^{(*/\prime)}$ [$e^+e^- \to K^+K^-$, $e^+e^- \to K\bar{K}^* + \text{c.c.}$, $e^+e^- \to K^{*+}K^{*-}$, $e^+e^- \to K_1(1270)^+K^-$, $e^+e^- \to K_1(1400)^+K^-$, $e^+e^- \to K_2^*(1430)\bar{K} + \text{c.c.}$, and $e^+e^- \to K(1460)^+K^-$]. In fact, the open-strange process from e^+e^- annihilation at center-of-mass energy $\sqrt{s} \sim 2$ GeV is mediated by different intermediate vector mesons. Since there is no isospin restriction, the highly excited ρ, ω, and ϕ meson states around 2 GeV may have contributions to the cross sections of the discussed open-strange processes, which makes the whole analysis quite complicated. Therefore, when facing the enhancement or dip structure around 2.2 GeV observed in both $e^+e^- \to K^+K^-$ and $e^+e^- \to K^+K^-\pi^0\pi^0$ [1,2], we see that it is a rough treatment to consider only a simple Breit-Wigner fit to the cross section data of the discussed open-strange processes from e^+e^- annihilation [1,2,19,20], which may inevitably lead to a puzzling situation mentioned above.

Obviously, we need to carry out a combined analysis to the present measured data of cross sections producing open-strange channels via e^+e^- annihilation [1,2,19,20], which is supported by the study of hadron spectroscopy. In fact, this approach was applied to construct higher charmonia above 4 GeV [21–23]. In this work, the hadron spectrum analysis is based on an unquenched potential model [21–27], by which we select suitable light vector mesons with mass around 2 GeV involved in the discussed processes. Of course, this mass spectrum analysis simultaneously provides the numerical spatial wave functions of the selected light vector mesons, which are applied to calculate their two-body open-strange decay widths and dilepton widths. With this preparation supported by the meson spectroscopy, the main task of the present work is to perform a combined analysis to the experimental cross section data of e^+e^- annihilations into open-strange channels, which can provide valuable information of light vector meson contributions to depict the experimental cross section data of e^+e^- annihilation into open-strange channels. Finally, we show later that the above puzzling situation can be clarified, which also provides a new perspective to construct the light vector meson family and understand the $Y(2175)$.

This paper is organized as follows. After the Introduction, we discuss the cross section of open-strange processes $e^+e^- \to K_{(J)}^{(*/\prime)}\bar{K}_{(J)}^{(*/\prime)}$ by considering the direct production and light vector meson contributions in Sec. II. Furthermore, we illustrate how to obtain the mass spectrum and decay behaviors of light vector mesons in Sec. III. In Sec. IV, based on our theoretical predictions for the branching ratios of the open-strange strong decay modes and dilepton widths of higher light vector mesons above 2 GeV, we find that higher light vector meson states play an important role to perform a combined analysis of the cross sections of e^+e^- annihilations into the open-strange processes. Finally, this work ends with a summary in Sec. V.

II. CROSS SECTIONS OF OPEN-STRANGE PROCESSES $e^+e^- \to K_{(J)}^{(*/\prime)}\bar{K}_{(J)}^{(*/\prime)}$ AROUND 2.0 GeV

In this section, we focus on the open-strange reactions $e^+e^- \to K^+K^-$ [1,19], $e^+e^- \to K\bar{K}^* + \text{c.c.}$ [20], $e^+e^- \to K^{*+}K^{*-}$ [2], $e^+e^- \to K_1(1270)^+K^-$ [2], $e^+e^- \to K_1(1400)^+K^-$ [2], $e^+e^- \to K_2^*(1430)\bar{K} + \text{c.c.}$ [20], and $e^+e^- \to K(1460)^+K^-$ [2] with center-of-mass (CM) energy around 2.0 GeV and illustrate how to present the cross section. In addition to the K^*K^*, $K_1(1270)K$, $K_1(1400)K$, and $K(1460)K$ channels measured by BESIII for the first time, there also exist the experimental results of several other open-strange channels, such as KK^* and $K_2(1430)^*K$, where their measured results were reported by the *BABAR* Collaboration in 2008 [20]. As shown in Fig. 1, there exist two mechanisms working together for the $e^+e^- \to K_{(J)}^{(*/\prime)}\bar{K}_{(J)}^{(*/\prime)}$ process. The first one is the direct

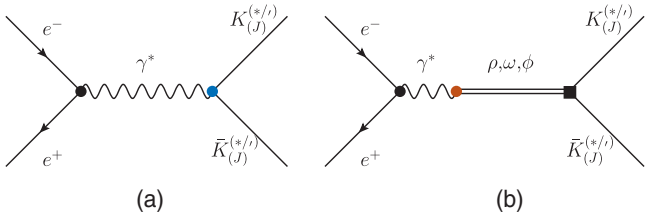

FIG. 1. The schematic diagrams for depicting the open-strange process $e^+e^- \to K^{(*/\prime)}_{(J)}\bar{K}^{(*/\prime)}_{(J)}$. Diagram (a) corresponds to a direct annihilation process, while diagram (b) is the resonance contributions from the intermediate ρ, ω, ϕ states.

annihilation of e^+e^- into open-strange channel, where the virtual photon directly couples with the final states $K^{(*/\prime)}_{(J)}\bar{K}^{(*/\prime)}_{(J)}$, which provides the background contribution. The second one occurs via the intermediate light vector meson states, which include the ρ-, ω-, and ϕ-like resonances.

Here, it is worth emphasizing that the kaonic final states $K_1(1270)$, $K_1(1400)$, $K(1460)$, and $K_2^*(1430)$ are assigned to strange meson states $K_1(1P_1)$, $K_1(1P_1')$, $K(2^1S_0)$, and $K_2(1^3P_2)$, respectively, where the unquenched modifications have been considered in Ref. [24]. The $K_1(1P_1)$ and $K_1(1P_1')$ are mixed states of two axial resonances $K_1(1^1P_1)$ and $K_1(1^3P_1)$. However, these kaonic states may have a more complicated structure than a quark-antiquark picture such as $K_1(1270)$, $K_1(1400)$, and $K(1460)$. In Ref. [28], the authors found that the invariant mass spectrum of $K^-\pi^+\pi^-$ of the process $K^-p \to K^-\pi^+\pi^-p$ can be reproduced well by considering $K_1(1270)$ as a molecular state from the vector-pseudoscalar meson interaction, which also supports two pole structures of $K_1(1270)$ [29]. For the $K(1460)$ state, the theoretical total width based on the $K(2^1S_0)$ explanation is larger than experimental data (see Ref. [24] for more details). In addition, the measured mass of $K(1460)$ is higher than that of $K^*(1410)$, which is a good candidate of $K(2^3S_1)$. Hence, several theorists claim that $K(1460)$ can be generated from the $KK\bar{K}$ and coupled channel dynamics [30–33]. Of course, we believe that these physical kaonic states should simultaneously contain the $s\bar{q}$ ($\bar{s}q$) configuration and other exotic components such as the molecular state from the interaction of different scattering channels. The concrete calculation of the impact of scattering channel dynamics on these strange mesons should be an interesting research topic in the future, which could be helpful to further improve our cross section analysis to the open-strange process of $e^+e^- \to KK_1(1270/1400)$.

In this work, the effective Lagrangian approach is adopted to calculate the discussed open-strange process $e^+e^- \to K^{(*/\prime)}_{(J)}\bar{K}^{(*/\prime)}_{(J)}$ as shown in Fig. 1. The effective Lagrangian densities involved in the concrete works include [34–38]

$$\begin{aligned}
\mathcal{L}_{KK\gamma} &= ieA^\mu(\bar{K}\partial_\mu K - \partial_\mu\bar{K}K),\\
\mathcal{L}_{KK^*\gamma} &= e\varepsilon^{\mu\nu\rho\sigma}\partial_\mu A_\nu(\bar{K}\partial_\rho K^*_\sigma + \partial_\rho\bar{K}^*_\sigma K),\\
\mathcal{L}_{K^*K^*\gamma} &= ie(A^\mu(\bar{K}^*_\nu \overleftrightarrow{\partial}_\mu K^{*\nu}) + \bar{K}^{*\mu}(K^*_\nu \overleftrightarrow{\partial}_\mu A^\nu)\\
&\quad + (A^\nu \overleftrightarrow{\partial}_\mu \bar{K}^*_\nu)K^{*\mu}),\\
\mathcal{L}_{KK_1\gamma} &= ieA_\mu(\bar{K}K_1^\mu - \bar{K}_1^\mu K),\\
\mathcal{L}_{KK_2\gamma} &= e\varepsilon_{\mu\nu\rho\sigma}\partial^\rho A^\sigma(\partial_\delta\bar{K}\partial^\mu K_2^{\nu\delta} + \partial^\mu\bar{K}_2^{\nu\delta}\partial_\delta K),\\
\mathcal{L}_{KK'\gamma} &= ieA^\mu(\bar{K}\overleftrightarrow{\partial}_\mu K' + \text{c.c.}),
\end{aligned} \tag{1}$$

$$\begin{aligned}
\mathcal{L}_{\gamma\mathcal{V}} &= \frac{-em_\mathcal{V}^2}{f_\mathcal{V}}\mathcal{V}_\mu A^\mu,\\
\mathcal{L}_{\mathcal{V}KK} &= ig_{\mathcal{V}KK}(\bar{K}\partial_\mu K - \partial_\mu\bar{K}K)\mathcal{V}^\mu,\\
\mathcal{L}_{\mathcal{V}KK^*} &= g_{\mathcal{V}KK^*}\varepsilon^{\mu\nu\rho\sigma}(\bar{K}\partial_\rho K^*_\sigma + \partial_\rho\bar{K}^*_\sigma K)\partial_\mu\mathcal{V}_\nu,\\
\mathcal{L}_{\mathcal{V}K^*K^*} &= ig_{\mathcal{V}K^*K^*}((\bar{K}^*_\nu \overleftrightarrow{\partial}_\mu K^{*\nu})\mathcal{V}^\mu + \bar{K}^{*\mu}(K^*_\nu \overleftrightarrow{\partial}_\mu \mathcal{V}^\nu)\\
&\quad + (\mathcal{V}^\nu \overleftrightarrow{\partial}_\mu \bar{K}^*_\nu)K^{*\mu}),\\
\mathcal{L}_{\mathcal{V}KK_1} &= ig_{\mathcal{V}KK_1}(\bar{K}K_1^\mu - \bar{K}_1^\mu K)\mathcal{V}_\mu,\\
\mathcal{L}_{\mathcal{V}KK_2} &= g_{\mathcal{V}KK_2}\varepsilon_{\mu\nu\rho\sigma}(\partial_\delta\bar{K}\partial^\mu K_2^{\nu\delta} + \partial^\mu\bar{K}_2^{\nu\delta}\partial_\delta K)\partial^\rho\mathcal{V}^\sigma,\\
\mathcal{L}_{\mathcal{V}KK'} &= ig_{\mathcal{V}KK'}(\bar{K}\overleftrightarrow{\partial}_\mu K' + \text{c.c.})\mathcal{V}^\mu,
\end{aligned} \tag{2}$$

where K_1, K_2, and K' stand for the kaon meson fields of $K_1(1270)/K_1(1400)$, $K_2^*(1430)$, and $K(1460)$, respectively, and $\mathcal{V}$ is the intermediate light vector meson field. Here, $g_{\mathcal{V}K^{(*/\prime)}_{(J)}K^{(*/\prime)}_{(J)}}$ is the corresponding coupling constants involved in the $\mathcal{V}$ state and the open-strange channel.

The scattering amplitudes of seven open-strange processes $e^+e^- \to KK$, $e^+e^- \to KK^*$, $e^+e^- \to K^*K^*$, $e^+e^- \to K_1(1270)K$, $e^+e^- \to K_1(1400)K$, $e^+e^- \to K_2^*(1430)K$, and $e^+e^- \to K(1460)K$ generally depicted in Fig. 1 can be written as

$$\begin{aligned}
\mathcal{M}^{KK^{(\prime)}}_{\text{Dir}} &= [\bar{v}(k_2)ie\gamma^\mu u(k_1)]\frac{-g_{\mu\nu}}{q^2}[-e(p_4^\nu - p_3^\nu)F_{KK^{(\prime)}}(q^2)],\\
\mathcal{M}^{KK^{(\prime)}}_{\mathcal{V}} &= [\bar{v}(k_2)ie\gamma_\mu u(k_1)]\frac{-g^{\mu\rho}}{q^2}\frac{-em_\mathcal{V}^2}{f_\mathcal{V}}\frac{-g_{\rho\nu} + q_\rho q_\nu/m_\mathcal{V}^2}{q^2 - m_\mathcal{V}^2 + im_\mathcal{V}\Gamma_\mathcal{V}}\\
&\quad \times [-g_{\mathcal{V}KK^{(\prime)}}(p_4^\nu - p_3^\nu)],
\end{aligned} \tag{3}$$

$$\begin{aligned}
\mathcal{M}^{KK^*}_{\text{Dir}} &= [\bar{v}(k_2)ie\gamma^\mu u(k_1)]\frac{-g_{\mu\nu}}{q^2}[e\varepsilon^{\alpha\nu\rho\sigma}q_\alpha p_{4\rho}\epsilon^*_{K^*\sigma}F_{KK^*}(q^2)],\\
\mathcal{M}^{KK^*}_{\mathcal{V}} &= [\bar{v}(k_2)ie\gamma_\mu u(k_1)]\frac{-g^{\mu\rho}}{q^2}\frac{-em_\mathcal{V}^2}{f_\mathcal{V}}\frac{-g_{\rho\nu} + q_\rho q_\nu/m_\mathcal{V}^2}{q^2 - m_\mathcal{V}^2 + im_\mathcal{V}\Gamma_\mathcal{V}}\\
&\quad \times [g_{\mathcal{V}KK^*}\varepsilon^{\alpha\nu\omega\sigma}q_\alpha p_{4\omega}\epsilon^*_{K^*\sigma}],
\end{aligned} \tag{4}$$

$$\mathcal{M}^{K^*K^*}_{\rm Dir} = [\bar{v}(k_2)ie\gamma^\mu u(k_1)]\frac{-g_{\mu\nu}}{q^2}[-e(g^{\alpha\beta}(p_4^\nu - p_3^\nu) - g^{\nu\beta}q^\alpha + g^{\nu\alpha}q^\beta + g^{\nu\alpha}p_3^\beta - g^{\nu\beta}p_4^\alpha)\epsilon^*_{K^*\alpha}\epsilon^*_{K^*\beta}F_{K^*K^*}(q^2)],$$

$$\mathcal{M}^{K^*K^*}_{\mathcal{V}} = [\bar{v}(k_2)ie\gamma_\mu u(k_1)]\frac{-g^{\mu\rho}}{q^2}\frac{-em_{\mathcal{V}}^2}{f_{\mathcal{V}}}\frac{-g_{\rho\nu}+q_\rho q_\nu/m_{\mathcal{V}}^2}{q^2-m_{\mathcal{V}}^2+im_{\mathcal{V}}\Gamma_{\mathcal{V}}} \times [-g_{\mathcal{V}K^*K^*}(g^{\alpha\beta}(p_4^\nu - p_3^\nu) - g^{\nu\beta}q^\alpha + g^{\nu\alpha}q^\beta + g^{\nu\alpha}p_3^\beta - g^{\nu\beta}p_4^\alpha)\epsilon^*_{K^*\alpha}\epsilon^*_{K^*\beta}], \quad (5)$$

$$\mathcal{M}^{KK_1}_{\rm Dir} = [\bar{v}(k_2)ie\gamma^\mu u(k_1)]\frac{-g_{\mu\nu}}{q^2}[ie\epsilon^{\nu*}_{K_1}F_{KK_1}(q^2)],$$

$$\mathcal{M}^{KK_1}_{\mathcal{V}} = [\bar{v}(k_2)ie\gamma_\mu u(k_1)]\frac{-g^{\mu\rho}}{q^2}\frac{-em_{\mathcal{V}}^2}{f_{\mathcal{V}}}\frac{-g_{\rho\nu}+q_\rho q_\nu/m_{\mathcal{V}}^2}{q^2-m_{\mathcal{V}}^2+im_{\mathcal{V}}\Gamma_{\mathcal{V}}} \times [ig_{\mathcal{V}KK_1}\epsilon^{\nu*}_{K_1}], \quad (6)$$

$$\mathcal{M}^{KK_2}_{\rm Dir} = [\bar{v}(k_2)ie\gamma^\mu u(k_1)]\frac{-g_{\mu\nu}}{q^2}[ie\varepsilon^{\alpha\beta\rho\nu}p_3^\delta q_\rho p_{4\alpha}\epsilon^*_{K_2\beta\delta} \times F_{KK_2}(q^2)],$$

$$\mathcal{M}^{KK_2}_{\mathcal{V}} = [\bar{v}(k_2)ie\gamma_\mu u(k_1)]\frac{-g^{\mu\rho}}{q^2}\frac{-em_{\mathcal{V}}^2}{f_{\mathcal{V}}}\frac{-g_{\rho\nu}+q_\rho q_\nu/m_{\mathcal{V}}^2}{q^2-m_{\mathcal{V}}^2+im_{\mathcal{V}}\Gamma_{\mathcal{V}}} \times [ig_{\mathcal{V}KK_2}\varepsilon^{\alpha\beta\omega\nu}p_3^\delta q_\omega p_{4\alpha}\epsilon^*_{K_2\beta\delta}], \quad (7)$$

where $q^\mu = (\sqrt{s},0,0,0)$, and p_3 and p_4 are the four-momenta of final states $K^{(*/\prime)}_{(J)}/\bar{K}^{(*/\prime)}_{(J)}$. Additionally, the timelike form factor $F_{K^{(*/\prime)}_{(J)}K^{(*/\prime)}_{(J)}}(q^2)$ is introduced when depicting the direct production process. Generally speaking, the expression of the form factor in the timelike region is relatively complicated. For simplicity, we adopt a universal form factor $F_{K^{(*/\prime)}_{(J)}K^{(*/\prime)}_{(J)}}(q^2) = f_{\rm Dir}e^{-aq^2}$ with free parameters $f_{\rm Dir}$ and a [39], which is an approximate description for the cross section of a direct production process in a narrow energy region between $\sqrt{s} = 2.0$–2.6 GeV. In addition, $m_{\mathcal{V}}$ and $\Gamma_{\mathcal{V}}$ are resonance parameters of the selected intermediate light vector meson states, which can be fixed by the corresponding experimental values or theoretical predictions. The total amplitude of $e^+e^- \to K^{(*/\prime)}_{(J)}\bar{K}^{(*/\prime)}_{(J)}$ can be written as the sum of a direct amplitude and different resonance contributions, i.e.,

$$\mathcal{M}^{K^{(*/\prime)}_{(J)}\bar{K}^{(*/\prime)}_{(J)}}_{\rm Total} = \mathcal{M}^{K^{(*/\prime)}_{(J)}\bar{K}^{(*/\prime)}_{(J)}}_{\rm Direct} + e^{i\theta_n}\sum_{\mathcal{V}_n}\mathcal{M}^{K^{(*/\prime)}_{(J)}\bar{K}^{(*/\prime)}_{(J)}}_{\mathcal{V}_n}, \quad (8)$$

where $\mathcal{V}_n$ stands for the selected intermediate vector resonances, and θ_n is the phase angle between the direct annihilation amplitude and the intermediate light vector meson contribution. With the above total amplitude, the cross section of $e^+e^- \to K^{(*/\prime)}_{(J)}\bar{K}^{(*/\prime)}_{(J)}$ can be calculated directly by

$$\sigma(e^+e^- \to K^{(*/\prime)}_{(J)}\bar{K}^{(*/\prime)}_{(J)}) = \int \frac{1}{64\pi s}\frac{1}{|p_{3\,\rm cm}|^2}\overline{\left|\mathcal{M}^{K^{(*/\prime)}_{(J)}\bar{K}^{(*/\prime)}_{(J)}}_{\rm Total}\right|^2}dt, \quad (9)$$

where $p_{3\,\rm cm}$ stands for the corresponding momentum of p_3 in the CM frame of a reaction.

Before depicting the cross section of our discussed open-strange processes, we need to select the suitable intermediate light vector meson states and investigate their resonance contributions, which can directly determine the coupling constants $g_{\mathcal{V}K^{(*/\prime)}_{(J)}K^{(*/\prime)}_{(J)}}$ and $f_{\mathcal{V}}$. In this work, we are mainly concerned with the CM energy region between 2.0 and 2.6 GeV. Consequently, how to obtain a mass spectrum of light vector mesons above 2.0 GeV is a crucial step before carrying out a theoretical analysis of the open-strange processes $e^+e^- \to K^{(*/\prime)}_{(J)}\bar{K}^{(*/\prime)}_{(J)}$. In the next section, we present the mass spectrum of light vector mesons by an unquenched quark model and discuss their decay behaviors.

III. MASS SPECTRUM AND DECAY BEHAVIORS OF LIGHT VECTOR MESONS

The mass spectrum of light vector mesons around 2.0 GeV has been studied by various potential models in the past several decades [40–45]. However, the results of the different models obviously differ from each other. Focusing on the excited strangeonium $\phi(3S)$ state that is considered to be a potential candidate of the $Y(2175)$, the analysis of the Regge trajectories indicates that its mass should be around 1.92 GeV [11]. However, Barnes *et al.* predicted a corresponding mass as 2.05 GeV [9]. In Ref. [45], the authors employed a covariant oscillator quark model with one gluon exchange effect, where the mass of the 3^3S_1 $s\bar{s}$ vector state is predicted to be 2.25 GeV. Therefore, obviously, there exists room for theorists to develop the phenomenological model to obtain a relatively reliable spectroscopy description of light vector mesons above 2.0 GeV.

For describing the highly excited light-flavor hadronic states, the relativistic effect and unquenched correction should be considered in the calculation. In this work, we adopt an unquenched relativized potential model to study the mass spectrum of light vector mesons, which has been widely applied to study other meson families from a kaon sector to a heavy quarkonium sector [21–27]. Here, we propose that the unquenched correction for the light vector meson family can be determined by other experimentally established S-wave and D-wave light meson families involving pion, ρ_2, and ρ_3, which could provide a relatively reliable scaling point for the energy region above 2.0 GeV in our theoretical model. Furthermore, the Okubo-Zweig-Iizuka (OZI)-allowed strong decay behaviors of these vector mesons can be obtained by the quark pair creation (QPC) model without β parameter dependence involved in

TABLE I. The mass spectra of the observed S-wave and D-wave light mesons calculated by the unquenched relativized potential model. Here, the comparison of the theoretical results and experimental data is given. All masses are in units of MeV.

Predicted states	Mass (The.)	Observed states	Mass (Expt.)
$\pi(1S)$	131	π	135 [3]
$\pi(2S)$	1265	$\pi(1300)$	1300 ± 100 [3]
$\pi(3S)$	1759	$\pi(1800)$	1810^{+9}_{-11} [3]
$\pi(4S)$	2115	$\pi(2070)$	2070 ± 35 [46]
$\pi(5S)$	2372	$\pi(2360)$	2360 ± 25 [46]
$\rho(1S)$	775	$\rho(770)$	775 [3]
$\rho(2S)$	1413	$\rho(1450)$	1465 ± 25 [3]
$\rho(3S)$	1862	$\rho(1900)$	1880 ± 30 [50]
$\omega(1S)$	775	$\omega(782)$	783 [3]
$\omega(2S)$	1413	$\omega(1420)$	1410 ± 60 [3]
$\pi_2(1D)$	1650	$\pi_2(1670)$	$1670.6^{+2.9}_{-1.6}$ [3]
$\pi_2(2D)$	2003	$\pi_2(2005)$	1963.6^{+17}_{-27} [3]
$\pi_2(3D)$	2278	$\pi_2(2285)$	$2285 \pm 20 \pm 25$ [47]
$\omega(1D)$	1633	$\omega(1650)$	1670 ± 30 [3]
$\rho(1D)$	1633	$\rho(1700)$	1720 ± 20 [3]
$\rho(2D)$	2003	$\rho(2000)$	2000 ± 30 [51]
$\rho_2(2D)$	2007	$\rho_2(1940)$	1940 ± 40 [48]
$\rho_2(3D)$	2284	$\rho_2(2225)$	2225 ± 35 [48]
$\rho_3(1D)$	1672	$\rho_3(1690)$	1688.8 ± 2.1 [3]
$\rho_3(2D)$	2013	$\rho_3(1990)$	1982 ± 14 [48]
$\rho_3(3D)$	2284	$\rho_3(2250)$	$2290 \pm 20 \pm 30$ [49]
$\phi(1S)$	1020	$\phi(1020)$	1019 [3]
$\phi(2S)$	1665	$\phi(1680)$	1680 ± 20 [3]

the simple harmonic oscillator (SHO) wave function necessary for calculating the transition matrix element, where we take the corresponding numerical meson wave function directly from our unquenched relativized potential model as input. For the convenience of the readers, we give a concise introduction to the method adopted in this work in Appendices A and B.

As pointed out in Ref. [23], the color screened effect is mainly reflected on the highly excited hadronic states, and so the key point of obtaining the reliable mass spectrum of light vector mesons above 2.0 GeV is to determine the screened parameter μ in the unquenched relativized potential model. In fact, the unquenched effect from the color screened interaction is a kind of nonperturbative behavior of QCD and is difficult to solve from a theoretical perspective, so its quantification needs the input of available experimental hints. At present, within the messy research situation of the light-flavor vector mesons, we believe that other light meson families could provide some valuable hints on our theoretical model.

In the quark model, in addition to an S-wave vector meson state, there still exist the corresponding vector D-wave partners, i.e., $n^{2S+1}L_J = n^3D_1$. Thus, as their spin singlet or triplet states, the experimental information of an S-wave pseudoscalar pion family and D-wave π_2, ρ_2, and ρ_3 states can help us determine the potential model parameters, where we notice that the masses of some highly excited states can reach around 2.3 GeV, such as $\pi(2360)$ [46], $\pi_2(2285)$ [47], $\rho_2(2225)$ [48], and $\rho_3(2250)$ [49]. Thus, these highly excited states play the role of the important scaling point of the color screened effect. The measured masses of these light-flavor mesons are summarized in Table I, which can be used to constrain three main screened confinement parameters and four relativistic correction factors ϵ_i. Based on a set of parameters listed in Table II, the global aspect of the light-flavor S-wave and D-wave meson mass spectra is well consistent with those of experiments, which can be clearly shown by the comparison between experimental values and our theoretical estimates in Table I. The screening parameter $\mu = 0.81$ indicates that the unquenched effect is indeed significant for describing the mass spectrum of light vector mesons.

TABLE II. Parameters in the unquenched relativized potential model adopted in this work.

Parameter[a]	Value	Parameter	Value
b (GeV^2)	0.229	c (GeV)	−0.300
$\epsilon_{\rm sos}$	0.973	ϵ_c	−0.164
$\epsilon_{\rm sov}$	0.262	ϵ_t	1.993
μ (GeV)	0.081		

[a]Generally, because the magnitude of unquenched effect is different in various meson systems, so different model parameters will be obtained by fitting respective meson mass spectrum.

With the above preparation, we can directly predict the mass spectrum and decay behavior of higher ρ, ω, and ϕ mesonic states above 2.0 GeV. In the QPC model, since the meson wave functions of initial and final states can be fixed by the corresponding eigenvectors solved from the above unquenched potential model, the partial width of each decay channel is only dependent on the parameter γ. However, it is worth noting that the corresponding

TABLE III. A comparison of the decay behavior of some well-established light vector mesons of the experimental average values and our theoretical estimate. Here, $\mathcal{B}_{e^+e^-}(\mathcal{V})$ and $\mathcal{B}_{h_1h_2}(\mathcal{V})$ represent the branching ratios $\Gamma(\mathcal{V} \to e^+e^-)/\Gamma^{\rm Total}_{\mathcal{V}}$ and $\Gamma(\mathcal{V} \to h_1h_2)/\Gamma^{\rm Total}_{\mathcal{V}}$, respectively.

Decay	Our	Expt. (Ave.) [3]
$\Gamma_{e^+e^-}(\rho(770))$ (keV)	6.98	7.04 ± 0.06
$\mathcal{B}_{e^+e^-}(\rho(1450))\mathcal{B}_{\omega\pi}(\rho(1450))$ $(\times 10^{-6})$	4.4	3.7 ± 0.4
$\mathcal{B}_{e^+e^-}(\rho(1450))\mathcal{B}_{\rho\eta}(\rho(1450))$ $(\times 10^{-6})$	0.60	0.58 ± 0.07
$\Gamma_{e^+e^-}(\omega(782))$ (keV)	0.78	0.60 ± 0.02
$\mathcal{B}_{e^+e^-}(\omega(1420))\mathcal{B}_{\omega\eta}(\omega(1420))$ $(\times 10^{-7})$	0.11	0.29 ± 0.15
$\mathcal{B}_{e^+e^-}(\omega(1420))\mathcal{B}_{\rho\pi}(\omega(1420))$ $(\times 10^{-7})$	2.74	6.58 ± 1.49
$\Gamma_{e^+e^-}(\phi(1020))$ (keV)	3.19	1.27 ± 0.04
$\mathcal{B}_{e^+e^-}(\phi(1680))\mathcal{B}_{KK^*}(\phi(1680))$ $(\times 10^{-7})$	20.4	22.2 ± 8.7
$\mathcal{B}_{e^+e^-}(\phi(1680))\mathcal{B}_{K^0\bar{K}^0}(\phi(1680))$ $(\times 10^{-7})$	1.37	1.31 ± 0.59

TABLE IV. The branching ratios of two-body open-strange strong decay and dilepton widths of ρ and ω meson states above 2.0 GeV. Here, the tiny branching ratio is marked as "···".

States	$\rho(2D)$	$\rho(4S)$	$\rho(3D)$	$\rho(5S)$	$\omega(2D)$	$\omega(4S)$	$\omega(3D)$	$\omega(5S)$
Mass (GeV)	2.003	2.180	2.283	2.422	2.003	2.180	2.283	2.422
$\Gamma_{e^+e^-}$ (keV)	0.020	0.063	0.016	0.036	0.0022	0.007	0.0018	0.004
Γ_{Total} (MeV)	179	102	158	80	181	104	94	69
$\mathcal{B}(KK)$	0.006	0.002	0.002	···	0.006	0.002	0.003	···
$\mathcal{B}(KK^*)$	0.001	···	···	···	0.001	···	···	···
$\mathcal{B}(K^*K^*)$	···	0.003	···	0.003	···	0.003	0.001	0.003
$\mathcal{B}(KK_1(1270))$	···	0.010	···	0.004	···	0.010	···	0.005
$\mathcal{B}(KK^*(1410))$	···	0.001	···	···	···	0.001	···	···
$\mathcal{B}(K^*K_1(1270))$	···	0.004	···	0.004	···	0.004	···	0.005
$\mathcal{B}(KK(1460))$	0.002	0.003	0.003	0.001	0.002	0.002	0.005	0.001

branching ratio is independent on any parameter because the γ in the numerator and the denominator cancel out each other. In addition, the dilepton widths of the higher vector states can also be related to the zero-point behavior of their radial wave functions, whose concrete width formula can be found in Refs. [40,52]. Thus, the production rates of intermediate light vector mesons in e^+e^- annihilations can also be estimated from a theoretical perspective. In Table III, we show the decay behavior comparison of some well-established light vector mesons between the experimental values and our theoretical results, which involve $\rho(770)$, $\rho(1450)$, $\omega(782)$, $\omega(1420)$, $\phi(1020)$, and $\phi(1680)$. It can be seen that our theoretical predictions are basically consistent with measured results, in a sense, which can prove the reliability of our models in estimating the decay properties of higher light vector meson states above 2.0 GeV. Of course, it is hard to evaluate the theoretical error magnitudes of these branching ratios for higher excited light vector meson states, but we think that the corresponding branching ratio predictions can be continuously tested by studying the cross section data of different reaction processes from electron-positron annihilation in addition to the open-strange process $e^+e^- \to K_J^{*\prime}\bar{K}_J^{*\prime}$ focused in this work, which can be left for future research.

The calculated mass spectrum and branching ratios of two-body open-strange strong decays as well as dilepton decay widths of $\rho(\omega)$ and ϕ meson states above 2.0 GeV are listed in Tables IV and V, respectively. There are eight light vector mesons existing near the energy region of $Y(2175)$, which include $\rho(2D)/\omega(2D)$, $\rho(4S)/\omega(4S)$, $\rho(3D)/\omega(3D)$, $\phi(3S)$, and $\phi(2D)$. However, it is almost impossible to study the present experimental data of open-strange channels by adding so many resonance contributions. Thus, we have to select the main intermediate resonances in our practical analysis. From the calculated numerical results, the dilepton widths of the isoscalar ω states are one order smaller than those of the isovector ρ partners, and their branching ratios to open-strange decay channels are almost the same. Furthermore, one can see that the branching ratios of $\phi(3S)/\phi(2D) \to K_{(J)}^{(*/\prime)}\bar{K}_{(J)}^{(*/\prime)}$ are far larger than those of $\rho(2D)$, $\rho(4S)$, and $\rho(3D)$, although there is no obvious difference among their production rates via electron-positron collisions. Therefore, we can conclude that the resonance contributions from the highly excited ρ and ω states can be safely ignored in studying the $e^+e^- \to K_{(J)}^{(*/\prime)}\bar{K}_{(J)}^{(*/\prime)}$ reaction above 2.0 GeV. Additionally, it is worth mentioning that the recently observed structure near 2.2 GeV in $e^+e^- \to K^+K^-$ by BESIII has been collected into "$\rho(2170)$" in the 2020 version of PDG [3], which should need a careful judgement and is not supported by our theoretical results here.

In Tables IV and V, we also give the theoretical total widths of the light vector mesons by taking a typical value of $\gamma = 6.57$ [10], which can be used as a reference. One can

TABLE V. The branching ratios of two-body open-strange strong decay and dilepton widths of ϕ mesons above 2.0 GeV. Additionally, the mass and decay behaviors of missing $\phi(1D)$ in experiments are also given. Here, the tiny branching ratio is marked as "···".

States	$\phi(1D)$	$\phi(3S)$	$\phi(2D)$	$\phi(4S)$	$\phi(3D)$
Mass (GeV)	1.860	2.103	2.236	2.423	2.519
$\Gamma_{e^+e^-}$ (keV)	0.063	0.106	0.017	0.050	0.010
Γ_{Total} (MeV)	515	156	265	140	171
$\mathcal{B}(KK)$	0.076	0.059	0.087	0.047	0.084
$\mathcal{B}(KK^*)$	0.100	0.242	0.067	0.145	0.050
$\mathcal{B}(K^*K^*)$	0.016	0.007	0.105	0.014	0.139
$\mathcal{B}(KK^*(1410))$	···	0.180	0.080	0.142	0.052
$\mathcal{B}(KK^*(1680))$	···	···	···	0.004	0.003
$\mathcal{B}(K^*K^*(1410))$	···	···	···	···	0.045
$\mathcal{B}(KK_2^*(1430))$	···	0.115	0.043	0.091	0.043
$\mathcal{B}(K^*K_2^*(1430))$	···	···	···	0.057	0.047
$\mathcal{B}(KK_1(1270))$	0.799	0.185	0.356	0.154	0.293
$\mathcal{B}(K^*K_1(1270))$	···	···	0.110	0.018	0.095
$\mathcal{B}(KK_1(1400))$	···	0.064	0.026	0.027	0.015
$\mathcal{B}(K^*K_1(1400))$	···	···	···	0.126	0.003
$\mathcal{B}(KK(1460))$	···	0.127	0.112	0.073	0.101
$\mathcal{B}(K^*K(1460))$	···	···	···	0.013	0.005
$\mathcal{B}(K^*K_0(1430))$	···	···	···	0.049	···
$\mathcal{B}(KK_3^*(1780))$	···	···	···	0.021	0.014

see that ϕ states play an absolutely dominant role in the open-strange processes from e^+e^- collisions, so three strangeonium states $\phi(3S)$, $\phi(2D)$, and $\phi(4S)$ are considered in our analysis. Utilizing the calculated decay behaviors of the higher strange quarkonium states presented in Table V, in the next section, we can directly decipher the cross sections of the present reported open-strange processes based on e^+e^- collisions.

IV. RESULTS OF NUMERICAL ANALYSIS

In the following, we fit the cross sections for seven open-strange reactions of $e^+e^- \to K^+K^-$ [1,19], $e^+e^- \to K\bar{K}^* +$ c.c. [20], $e^+e^- \to K^{*+}K^{*-}$ [2], $e^+e^- \to K_1(1270)^+K^-$ [2], $e^+e^- \to K_1(1400)^+K^-$ [2], $e^+e^- \to K_2^*(1430)\bar{K} +$ c.c. [20], and $e^+e^- \to K(1460)^+K^-$ [2], which provide us direct evidence to demonstrate the nature of the vector structure around 2.2 GeV observed in these processes. It is worth mentioning that although the contributions from resonances $\phi(1020)$, $\phi(1680)$, and $\phi(1D)$ in the energy region above 2.0 GeV are obviously suppressed compared with those at their resonant peak positions, they still may play a significant background role in some specific open-strange channels, which have to be included in our analysis. According to the corresponding decay behaviors presented in Tables III and V, we consider the contributions of lower $\phi(1020)$, $\phi(1680)$, and $\phi(1D)$ in reaction channels KK, $KK^{(*)}$, and $KK_1(1270)$, respectively. The resonance masses and total widths of $\phi(1020)$ and $\phi(1680)$ can be fixed by the experimental average values in PDG [3]. All coupling constants $g_{\phi K_{(J)}^{(*/\prime)} K_{(J)}^{(*/\prime)}}/f_\phi$ in Eqs. (3)–(7) can be related to the corresponding products of $\Gamma(\phi \to e^+e^-) \times \mathcal{B}(\phi \to K_{(J)}^{(*/\prime)} \bar{K}_{(J)}^{(*/\prime)})$ by the following expressions:

$$
\begin{aligned}
\frac{g_{\phi KK}}{f_\phi} &= \sqrt{\frac{288\pi^2\Gamma_\phi m_\phi \Gamma(\phi \to e^+e^-)\mathcal{B}(\phi \to K\bar{K})}{e^4\lambda(m_\phi, m_K, m_K)^{\frac{3}{2}}}},\\
\frac{g_{\phi KK^*}}{f_\phi} &= \sqrt{\frac{144\pi^2\Gamma_\phi \Gamma(\phi \to e^+e^-)\mathcal{B}(\phi \to K\bar{K}^* + \text{c.c.})}{e^4\lambda(m_\phi, m_K, m_{K^*})^{\frac{3}{2}} m_\phi}},\\
\frac{g_{\phi K^*K^*}}{f_\phi} &= \sqrt{\frac{288\pi^2\Gamma_\phi m_\phi \Gamma(\phi \to e^+e^-)\mathcal{B}(\phi \to K^*\bar{K}^*)}{e^4\lambda(m_\phi, m_{K^*}, m_{K^*})^{\frac{3}{2}}(m_\phi^4 - 4m_\phi^2 m_{K^*}^2 + 12m_{K^*}^4)}},\\
\frac{g_{\phi KK_1}}{f_\phi} &= \sqrt{\frac{144\pi^2\Gamma_\phi m_\phi \Gamma(\phi \to e^+e^-)\mathcal{B}(\phi \to K\bar{K}_1 + \text{c.c.})}{e^4\lambda(m_\phi, m_K, m_{K_1})^{\frac{1}{2}}}},\\
\frac{g_{\phi KK_2}}{f_\phi} &= \sqrt{\frac{144\pi^2\Gamma_\phi \Gamma(\phi \to e^+e^-)\mathcal{B}(\phi \to K\bar{K}_2 + \text{c.c.})}{e^4\lambda(m_\phi, m_K, m_{K_2})^{\frac{5}{2}} m_\phi^3 m_\phi^2}},\\
\frac{g_{\phi KK'}}{f_\phi} &= \sqrt{\frac{144\pi^2\Gamma_\phi m_\phi \Gamma(\phi \to e^+e^-)\mathcal{B}(\phi \to K\bar{K}' + \text{c.c.})}{e^4\lambda(m_\phi, m_K, m'_K)^{\frac{3}{2}}}},
\end{aligned}
\tag{10}
$$

where $\lambda(x, y, z) = x^2 + y^2 + z^2 - 2xy - 2xz - 2yz$ is the Källen function. Thus, the only fitting parameters are relative phase angles and f_{Dir} and a in a direct production amplitude. However, in a practical analysis, we find that the fitted χ^2 value is obviously dependent on resonance parameters of three strange quarkonium states $\phi(3S)$, $\phi(2D)$, and $\phi(4S)$. At the same time, combining the fact that the measured errors of experimental resonance parameters of most of light-flavor mesons are generally large as seen in Table I, the masses of $m_{\phi(3S)}$, $m_{\phi(2D)}$, $m_{\phi(4S)}$, and strong decay parameter γ can be set as free parameters, which should vary around their fixed theoretical values.

The combined fit to seven open-strange processes from e^+e^- collisions mentioned above is presented in Fig. 2. Benefiting from the calculated decay behaviors of light vector mesons in Sec. III, the contributions of each individual light vector meson to the cross sections of different open-strange processes can be directly obtained, which are also shown in Fig. 2. One can see that experimental cross sections of the measured open-strange processes can be described well by introducing the resonance contributions from highly excited $3S$, $2D$, and $4S$ strange quarkonium states, and a combined $\chi^2/\text{d.o.f} = 2.29$ is obtained. Especially, the apparent enhancement or dip around 2.2 GeV seen in $e^+e^- \to K^+K^-$, $K(1460)^+K^-$, $K_1(1270)^+K^-$, $K_1(1400)^+K^-$, and $K_2^*(1430)\bar{K} +$ c.c. can be completely reproduced via the interference effect from the resonance contributions of $\phi(3S)$ and $\phi(2D)$ and the continuum background, where an S-wave state plays a dominant role. Here, it is worth mentioning that the $e^+e^- \to K^*\bar{K}_1(1270) +$ c.c. could be an excellent reaction process to detect the dominant signal of a D-wave state, where the contribution from a $3S$ state is suppressed as shown in Table V. Based on the interference effect, we can naturally explain why there exists an inconsistent peak position of the observed vector structure around 2.2 GeV among different reaction channels, such as KK channel in Fig. 2(a) and other channels in Figs. 2(c)–2(f). Here, we can see that a simple Breit-Wigner fit to the corresponding cross section is indeed a very rough treatment.

Here, it is worth mentioning that the coupling constants $g_{\phi KK_1(1270)}$ and $g_{\phi KK_1(1400)}$ depend on the mixing angle between $K_1(1^1P_1)$ and $K_1(1^3P_1)$. Based on a same unquenched potential model, the mixing angle θ_{1P} was found to be limited in the range of 41.5°–48° by fitting relevant experimental data in Ref. [24]. In order to further investigate the impact of this mixing angle on the corresponding cross section analysis, we give the dependence of branching ratios $\mathcal{B}(\phi(3S/2D/4S) \to KK_1(1270/1400))$ on the mixing angle θ_{1P} in Fig. 3. It can be seen that there are no significant changes in the branching ratio results, so we adopt the center value of $\theta_{1P} = 45°$ in the above cross section analysis.

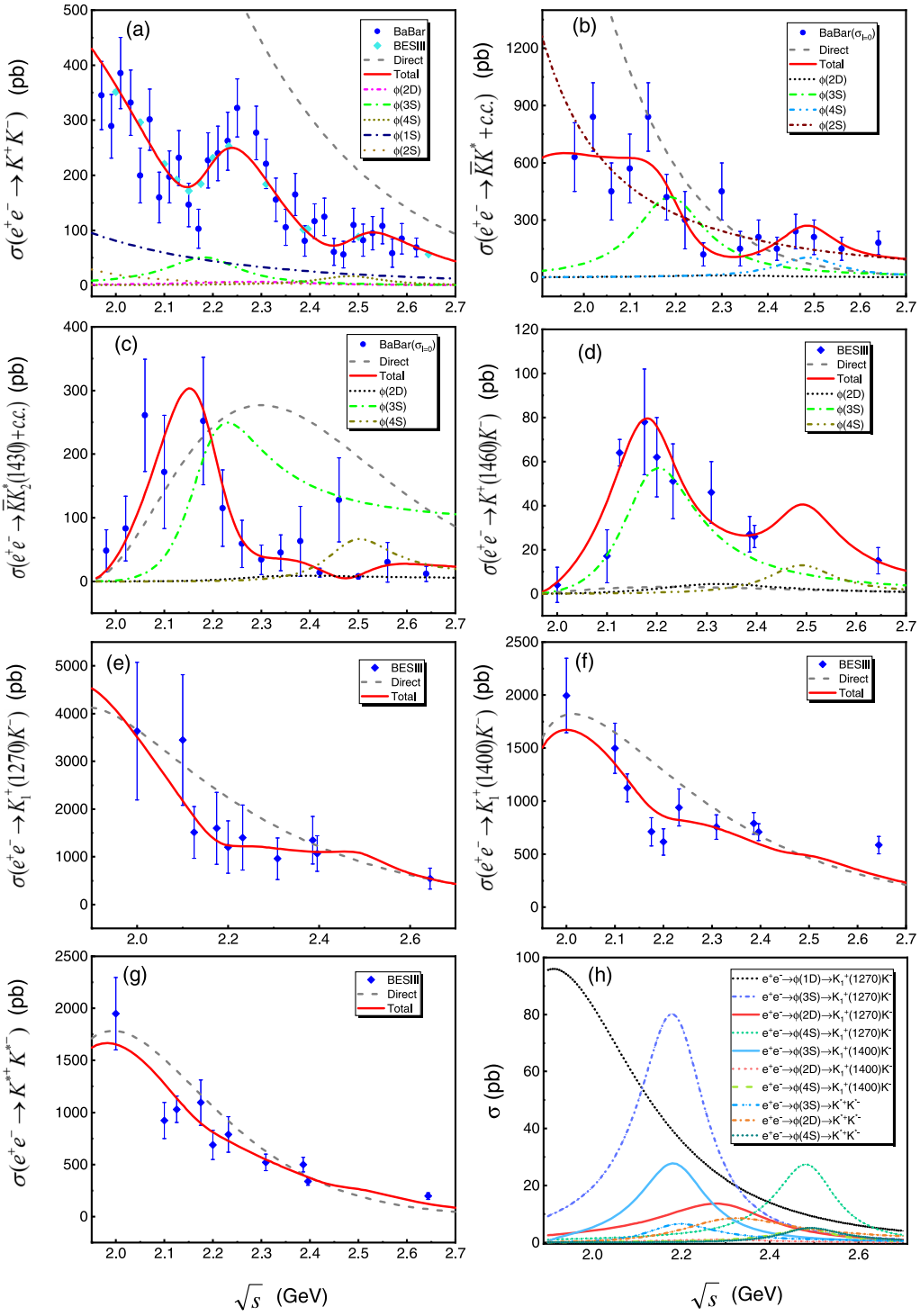

FIG. 2. The combined analysis to seven open-strange processes from e^+e^- collisions [1,2,19,20], which are shown in panels (a)–(g), successively. Here, $\sigma_{I=0}$ in panels (b) and (c) means that the measured cross section of the reaction process corresponds to the isoscalar component.

The obtained phase angles and direct production parameters of each process in the combined fit are summarized in Table VI. In addition, the resonance masses and widths of $\phi(3S)$, $\phi(2D)$, and $\phi(4S)$ are fitted to be

$$m_{\phi(3S)} = 2183 \pm 1 \text{ MeV}, \quad \Gamma_{\phi(3S)} = 185 \pm 4 \text{ MeV},$$
$$m_{\phi(2D)} = 2290 \pm 3 \text{ MeV}, \quad \Gamma_{\phi(2D)} = 312 \pm 6 \text{ MeV},$$
$$m_{\phi(4S)} = 2485 \pm 5 \text{ MeV}, \quad \Gamma_{\phi(4S)} = 165 \pm 3 \text{ MeV},$$

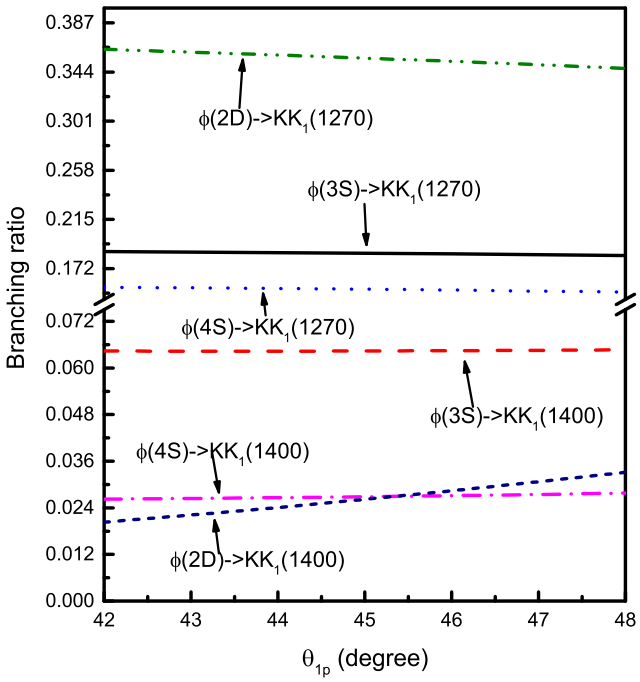

FIG. 3. The dependence of branching ratio $\mathcal{B}(\phi(3S/2D/4S) \to KK_1(1270/1400))$ on the mixing angle θ_{1P} between $K_1(1^1P_1)$ and $K_1(1^3P_1)$.

respectively. The above results indicate that both $\phi(3S)$ and $\phi(2D)$ are broad states, which are consistent with previous theoretical calculations [9–12]. As mentioned in the Introduction, the measured resonance width of $Y(2175)$ is narrower than predictions for $\phi(3S)$ or $\phi(2D)$. From Fig. 2, it can be seen that this width problem can also be explained in our theoretical analysis of considering the interference effect among two light vector meson contributions as well as a background term. Here, if we fit the cross sections in Figs. 2(a) or 2(c)–2(f) by a simple Breit-Wigner formula, we would obtain the narrow width around 100 MeV.

Additionally, we notice that the experimental data of reaction $e^+e^- \to K^{*+}K^{*-}$ in Fig. 2(g) does not show an obvious signal for the existence of a vector structure around 2.2 GeV. Here, we want to emphasize that this interesting phenomenon can also be understood in our theoretical framework. From Table V, we can find a branching ratio $\mathcal{B}(\phi(3S) \to K^*\bar{K}^*) = 7 \times 10^{-3}$, which is obviously smaller than those of other open-strange decay channels. The reason for this is that there exists a node effect for the overlap integral among the wave functions of the initial $\phi(3S)$ state and final state $K^*\bar{K}^*$. From Fig. 2(h), it can be seen that these resonance contributions in process $e^+e^- \to K^{*+}K^{*-}$ are of the order of several pb, which is far lower than a direct continuum. Therefore, this is strong evidence to support our explanation of the vector structure around 2.2 GeV observed in open-strange processes. In conclusion, our theoretical analysis can well clarify the present puzzling situation in understanding the cross section of open-strange processes from e^+e^- annihilation without adding any unknown resonance contributions, which means that this work provides a new opinion to construct the light vector meson family and understand the $Y(2175)$.

Finally, we would like to suggest that our experimental colleagues search for a predicted new resonance structure $\phi(4S)$ around 2.5 GeV, whose signal can be discovered by several typical open-strange processes $e^+e^- \to K\bar{K}$, $e^+e^- \to K\bar{K}^* + \text{c.c.}$, and $e^+e^- \to K\bar{K}(1460) + \text{c.c.}$ as presented in Fig. 2, especially for the $KK(1460)$ channel, where the experimental data on relevant energy region is still lacking. This should be an interesting research topic for future BESIII and BelleII experiments.

V. SUMMARY

Recently, the BESIII Collaboration performed precise measurements of cross sections for open-strange processes $e^+e^- \to K^+K^-$ [1] and $e^+e^- \to K^+K^-\pi^0\pi^0$ [2], where a clear structure around 2.2 GeV was observed. This is the first certain evidence for the existence of the vector structure around 2.2 GeV in open-strange reaction processes. The experimental resonance masses and widths of this newly observed vector structure are found to be consistent with those of the $Y(2175)$ first reported in the hidden-strange reaction $e^+e^- \to \phi f_0(980) \to \phi\pi^+\pi^-$ by the *BABAR* Collaboration in 2006 [4]. Thus, this simple comparison seems to imply that this structure around

TABLE VI. The fitted parameters in the combined analysis to the experimental data of seven open-strange processes from e^+e^- collisions. The listed phase angles θ_ϕ are in units of radian.

Processes	f_{Dir}	a (GeV^{-2})	$\theta_{\phi(1S)}$	$\theta_{\phi(2S)}$	$\theta_{\phi(1D)}$	$\theta_{\phi(3S)}$	$\theta_{\phi(2D)}$	$\theta_{\phi(4S)}$
$e^+e^- \to K^+K^-$	-0.29	0.33	6.09 ± 0.04	0.52 ± 0.06	⋯	2.54 ± 0.02	5.77 ± 0.05	2.80 ± 0.05
$e^+e^- \to K\bar{K}^* + \text{c.c.}$	1.95 ± 0.07	0.85 ± 0.01	⋯	3.51 ± 0.10	⋯	2.74 ± 0.17	1.32 ± 0.41	4.84 ± 0.38
$e^+e^- \to K^{*+}K^{*-}$	-2.68 ± 0.05	0.89 ± 0.01	⋯	⋯	⋯	2.14 ± 0.47	2.57 ± 0.36	3.05 ± 0.49
$e^+e^- \to K_1(1270)^+K^-$	0.78 ± 0.07	0.22 ± 0.01	⋯	⋯	2.47 ± 0.52	5.02 ± 0.63	4.87 ± 1.10	1.28 ± 0.95
$e^+e^- \to K_1(1400)^+K^-$	0.87 ± 0.16	0.28 ± 0.04	⋯	⋯	⋯	4.62 ± 0.21	5.79 ± 0.65	6.28 ± 0.33
$e^+e^- \to K_2^*(1430)\bar{K} + \text{c.c.}$	1.09 ± 0.11	0.80 ± 0.02	⋯	⋯	⋯	3.54 ± 0.10	1.11 ± 0.51	4.67 ± 0.24
$e^+e^- \to K(1460)^+K^-$	-0.12 ± 0.22	0.46 ± 0.35	⋯	⋯	⋯	6.22 ± 0.18	5.55 ± 0.64	6.26 ± 1.30

2.2 GeV may be the same state as $Y(2175)$. In the past years, the popular theoretical explanations of $Y(2175)$ mainly include the hybrid $s\bar{s}g$ [8], vector strangeonium state $\phi(3S)$ [9,10], and $\phi(2D)$ [10–12], which are just favored by the open-strange channels. However, the theoretical studies on their decay behaviors [8–12,15–18] definitely indicate that it is difficult to understand the experimental data of these open-strange reactions [1,2] either under the hybrid or strangeonium assignment to the $Y(2175)$. This means that there are no appropriate theoretical pictures to convincingly explain this newly observed vector structure around 2.2 GeV.

In order to clarify this puzzling situation, we have pointed out that it is not an easy task to analyze the cross sections of the open-strange processes from e^+e^- annihilations, where both highly excited and light vector meson ρ, ω, and ϕ states may have significant contributions. Thus, a simple Breit-Wigner fit to the signal around 2.2 GeV observed in the cross sections of open-strange processes must be a very rough treatment. Based on this motivation, in this work, we have performed a combined analysis to the cross sections of seven reported open-strange reactions of $e^+e^- \to K^+K^-$ [1,19], $e^+e^- \to K\bar{K}^* + \text{c.c.}$ [20], $e^+e^- \to K^{*+}K^{*-}$ [2], $e^+e^- \to K_1(1270)^+K^-$ [2], $e^+e^- \to K_1(1400)^+K^-$ [2], $e^+e^- \to K_2^*(1430)\bar{K} + \text{c.c.}$ [20], and $e^+e^- \to K(1460)^+K^-$ [2] by introducing the light vector meson contributions, which is supported by the study of hadron spectroscopy. Here, we have employed an unquenched relativized potential model [21–27] to study the mass spectra and wave functions of light vector meson states. By taking the exact numerical wave functions from the potential model as input, the dilepton widths and the branching ratios of open-strange decay channels of light vector mesons can be estimated without any parameter dependence. Based on these available theoretical results, the cross sections of the seven open-strange reactions are found to be well described by considering the direct production and the light vector meson contributions. Furthermore, we have demonstrated that the observed vector structure around 2.2 GeV in these open-strange channels does not correspond to a single resonance, and it can be identified as an interference signal from highly excited strange quarkonium states $\phi(3S)$ and $\phi(2D)$, by which the present puzzling situations can be naturally clarified. From this practical example in this work, we have actually provided a new perspective to construct the light vector meson family and understand the $Y(2175)$, which can continue to be tested in hidden-strange channels and other related processes. These should be helpful to solve the messy research situation of light vector mesons around 2.2 GeV thoroughly in the future.

In the full hadron spectrum, the light meson spectroscopy has a particular position because there exist abundant experimental data in the energy region of light mesons. In addition to the intriguing vector structure around 2.2 GeV, we have also predicted a new strange quarkonium structure $\phi(4S)$ near $\sqrt{s} = 2.5$ GeV, whose mass and total width are predicted to be $m_{\phi(4S)} = 2485 \pm 5$ MeV and $\Gamma_{\phi(4S)} = 165 \pm 3$ MeV, respectively. The establishment of this particle in experiments is very important for further constructing the light vector meson family. This should be a challenging task to the experimentalist community and is worth working in the future.

ACKNOWLEDGMENTS

The authors would like to thank Dr. Wen-Biao Yan and Ya-Teng Zhang for useful discussions. This work is supported by the China National Funds for Distinguished Young Scientists under Grant No. 11825503, National Key Research and Development Program of China under Contract No. 2020YFA0406400, 111 Project under Grant No. B20063, and National Natural Science Foundation of China under Grant No. 12047501. J. Z. Wang is also supported by Education Department of Gansu Province for Excellent Graduate Student "Innovation Star" under Grant No. 2021CXZX-013.

APPENDIX A: A CONCISE REVIEW OF THE UNQUENCHED RELATIVIZED POTENTAIL MODEL

The Hamiltonian depicting the interaction between the quark and antiquark in the unquenched relativized potential model is described as [21–27,40]

$$\tilde{H} = \tilde{H}_0 + \tilde{V}_{\text{eff}}(\mathbf{p}, \mathbf{r}), \tag{A1}$$

with

$$\tilde{H}_0 = \sqrt{m_q^2 + \text{p}^2} + \sqrt{m_{\bar{q}}^2 + \text{p}^2}, \tag{A2}$$

where m_q and $m_{\bar{q}}$ denote the constituent masses of the light quark and antiquark, respectively. In our calculation, the quark masses $m_u = m_d = 0.22$ GeV and $m_s = 0.424$ GeV are taken. The effective potential of the $q\bar{q}$ interaction contains three parts, i.e.,

$$\tilde{V}_{\text{eff}}(\mathbf{p}, \mathbf{r}) = \tilde{H}^{\text{conf}} + \tilde{H}^{\text{so}} + \tilde{H}^{\text{hyp}}, \tag{A3}$$

where the confinement interaction $\tilde{H}^{\text{conf}}$ includes a short $\gamma^\mu \otimes \gamma_\mu$ one-gluon exchange interaction and an unquenched confining interaction. In the nonrelativistic limit, the effective potential can be written as the standard nonrelativistic expression, i.e.,

$$V_{\text{eff}}(\mathbf{p}, \mathbf{r}) = H^{\text{conf}} + H^{\text{so}} + H^{\text{hyp}}, \tag{A4}$$

with

$$H^{\rm conf} = \left[-\frac{3}{4}\left(c + \frac{b(1-e^{-\mu r})}{\mu}\right) + \frac{\alpha(r)}{r}\right](\boldsymbol{F_q}\cdot\boldsymbol{F_{\bar q}}) = S(r) + G(r), \tag{A5}$$

where $H^{\rm conf}$ contains the spin-independent color screened confinement $S(r) = c + b(1-e^{-\mu r})/\mu$ and Coulomb-type interaction $G(r) = \alpha(r)/r$. Here, $\boldsymbol{F}$ is related to the Gell-Mann matrices in color space, and $\langle \boldsymbol{F_q}\cdot\boldsymbol{F_{\bar q}}\rangle = -4/3$ is taken in meson system. The third term $H^{\rm hyp}$ is the color-hyperfine interaction and reads as

$$H^{\rm hyp} = -\frac{\alpha_s(r)}{m_q m_{\bar q}}\left[\frac{8\pi}{3}\mathbf{S_q}\cdot\mathbf{S_{\bar q}}\delta^3(\mathbf{r}) + \frac{1}{r^3}\left(\frac{3\mathbf{S_q}\cdot\mathbf{r}\mathbf{S_{\bar q}}\cdot\mathbf{r}}{r^2} - \mathbf{S_q}\cdot\mathbf{S_{\bar q}}\right)\right](\boldsymbol{F_q}\cdot\boldsymbol{F_{\bar q}}). \tag{A6}$$

The second term $H^{\rm so} = H^{\rm so(cm)} + H^{\rm so(tp)}$ in Eq. (A4) is the spin-orbit interaction with the color magnetic term resulting from one-gluon exchange,

$$H^{\rm so(cm)} = -\frac{\alpha_s(r)}{r^3}\left(\frac{1}{m_q} + \frac{1}{m_{\bar q}}\right)\left(\frac{\mathbf{S_q}}{m_q} + \frac{\mathbf{S_{\bar q}}}{m_{\bar q}}\right)\cdot\boldsymbol{L}(\boldsymbol{F_q}\cdot\boldsymbol{F_{\bar q}}), \tag{A7}$$

and Thomas precession term,

$$H^{\rm so(tp)} = -\frac{1}{2r}\frac{\partial H^{\rm conf}}{\partial r}\left(\frac{\mathbf{S_q}\cdot\boldsymbol{L}}{m_q^2} + \frac{\mathbf{S_{\bar q}}\cdot\boldsymbol{L}}{m_{\bar q}^2}\right). \tag{A8}$$

In the above expressions, $\mathbf{S_q}$ and $\mathbf{S_{\bar q}}$ denote the spin of the light flavor quark and antiquark, respectively, while $\boldsymbol{L}$ is the orbital momentum between two quarks inside the meson.

The relativistic effect is introduced in two ways (see Ref. [40] for more details). First, considering the effects of internal motion inside a light hadron and the nonlocality interactions between a light quark and antiquark, a smearing function could be introduced, i.e.,

$$\rho(\boldsymbol{r}-\boldsymbol{r'}) = \frac{\sigma_{12}^3}{\pi^{3/2}}e^{-\sigma_{12}^2(\boldsymbol{r}-\boldsymbol{r'})^2}, \tag{A9}$$

with

$$\sigma_{12}^2 = \sigma_0^2\left[\frac{1}{2} + \frac{1}{2}\left(\frac{4m_q m_{\bar q}}{(m_q+m_{\bar q})^2}\right)^4\right] + s^2\left(\frac{2m_q m_{\bar q}}{m_q+m_{\bar q}}\right)^2, \tag{A10}$$

where $\sigma_0 = 1.8$ GeV and $s = 3.88$ GeV are constant. Hence, the unquenched confinement potential $S(r)$ and one-gluon exchange interaction $G(r)$ become a smeared potential $\tilde S(r)$ and $\tilde G(r)$ by the general transformation

$$\tilde f(r) = \int d^3r'\rho(\boldsymbol{r}-\boldsymbol{r'})f(r'). \tag{A11}$$

In addition, a relativized potential should depend on quark momentum, which can be taken into account by introducing a momentum-dependent factor. So the Coulomb term $\tilde G(r)$ and the contact, tensor, vector spin-orbital, and scalar spin-orbital potential $\tilde V_i(r)$ could be modified as

$$\tilde G(r) \to \left(1 + \frac{p^2}{E_q E_{\bar q}}\right)^{1/2}\tilde G(r)\left(1 + \frac{p^2}{E_q E_{\bar q}}\right)^{1/2}, \quad \frac{\tilde V_i(r)}{m_q m_{\bar q}} \to \left(\frac{m_q m_{\bar q}}{E_q E_{\bar q}}\right)^{1/2+\epsilon_i}\frac{\tilde V_i(r)}{m_q m_{\bar q}}\left(\frac{m_q m_{\bar q}}{E_q E_{\bar q}}\right)^{1/2+\epsilon_i}, \tag{A12}$$

where E_q ($E_{\bar q}$) is the energy of quark (antiquark), and ϵ_i denotes a momentum correction parameter with different types of interactions in Eqs. (A6)–(A8). One may see that the momentum-dependent factor returns to unity in the nonrelativistic limit.

By diagonalizing the Hamiltonian in Eq. (A1) with a series of the SHO basis, the obtained eigenvalues and eigenvectors can correspond to the meson mass and wave function, respectively. In the momentum space, the general form of an SHO wave function is

$$\Psi_{nLM_L}(\mathbf{p}) = R_{nL}(p,\beta)Y_{LM_L}(\boldsymbol{\Omega}_p), \tag{A13}$$

with

$$R_{nL}(p,\beta) = \frac{(-1)^n(-i)^L}{\beta^{3/2}}e^{-\frac{p^2}{2\beta^2}}\sqrt{\frac{2n!}{\Gamma(n+L+3/2)}}\left(\frac{p}{\beta}\right)^L \times L_n^{L+1/2}\left(\frac{p^2}{\beta^2}\right), \tag{A14}$$

where $R_{nL}(p,\beta)$ is a radial wave function of a harmonic oscillator, $Y_{LM_L}(\boldsymbol{\Omega}_p)$ a spherical harmonic function, and $L_n^{L+1/2}(x)$ the associated Laguerre polynomial.

APPENDIX B: QUARK PAIR CREATION MODEL

The quark pair creation model [53,54] is usually applied to study the OZI-allowed two-body strong decays of a hadronic state, which are absolutely dominant decay modes for the meson or baryon state above the decay threshold. In the following, we give a brief introduction of the QPC model. When a meson decays, a quark-antiquark pair created from the vacuum with the quantum number $J^{PC} = 0^{++}$ has a connection with the antiquark and quark inside the initial meson to produce two final mesons. The decay matrix element of this process $A \to BC$ can be written as $\langle BC|\mathcal{T}|A\rangle = \delta^3(\mathbf{P}_B + \mathbf{P}_C)\times\mathcal{M}^{M_{J_A}M_{J_B}M_{J_C}}(\mathbf{P})$, where the transition operator $\mathcal{T}$ represents a quark-antiquark pair

creation from the vacuum. Taking particle A as an example, the wave function of the mock state (A, B, C) is defined as [53,54]

$$\begin{aligned}&|A(n_A^{2S_A+1}L_{AJ_AM_{J_A}})(\boldsymbol{P}_A)\rangle\\&\equiv\sum_{M_{L_A},M_{S_A}}\langle L_AM_{L_A}S_AM_{S_A}|J_AM_{J_A}\rangle\\&\times\sqrt{2E_A}\int d^3\boldsymbol{p}_A\psi_{n_AL_AM_{L_A}}(\boldsymbol{p}_A)\chi^{12}_{S_AM_{S_A}}\phi^{12}_A\omega^{12}_A\\&\times\left|q_1\left(\frac{m_1}{m_1+m_2}\boldsymbol{P}_A+\boldsymbol{p}_A\right)\bar{q}_2\left(\frac{m_2}{m_1+m_2}\boldsymbol{P}_A+\boldsymbol{p}_A\right)\right\rangle,\end{aligned}\tag{B1}$$

where m_1 and m_2 are masses of quark q_1 and antiquark $\bar{q}_2$, respectively, n_A is the radial quantum number of a meson A. Here, $\boldsymbol{S}_A$ and $\boldsymbol{L}_A$ are spin $\boldsymbol{S}_q+\boldsymbol{S}_{\bar{q}}$ and relative orbital angular momentum between q_1 and $\bar{q}_2$, respectively. $\boldsymbol{J}_A=\boldsymbol{S}_A+\boldsymbol{L}_A$ is the total spin, while $\boldsymbol{P}_A=\boldsymbol{p}_1+\boldsymbol{p}_2$ and E_A are CM momentum and energy, respectively. $\boldsymbol{p}_A=\frac{m_1\boldsymbol{p}_1-m_2\boldsymbol{p}_2}{m_1+m_2}$ denotes the relative momentum between q_1 and $\bar{q}_2$. $\chi^{12}_{S_AM_{S_A}}$, ϕ^{12}_A, ω^{12}_A, and $\psi_{n_AL_AM_{L_A}}(\boldsymbol{p}_A)$ are the spin, flavor, color, and spatial wave function of a meson A, respectively. The total decay width of $A\to BC$ in the CM frame is given by

$$\Gamma_{A\to BC}=\frac{\pi}{4}\frac{|\mathbf{P}|}{m_A^2}\sum_{JL}|\mathcal{M}^{JL}(\mathbf{P})|^2.\tag{B2}$$

Here, $\mathbf{P}=\mathbf{P}_B=-\mathbf{P}_C$. $\boldsymbol{L}$ and $\boldsymbol{J}$ denote the relative orbital angular and total spin momentum between final states B and C, respectively. $\mathcal{M}^{JL}(\mathbf{P})$ is the partial wave amplitude, which can be directly related to the helicity amplitude $\mathcal{M}^{M_{J_A}M_{J_B}M_{J_C}}(\mathbf{P})$ according to the Jacob-Wick formula [55]. In the CM frame, the specific form of $\mathcal{M}^{M_{J_A}M_{J_B}M_{J_C}}(\mathbf{P})$ can be written as

$$\begin{aligned}\mathcal{M}^{M_{J_A}M_{J_B}M_{J_C}}(\mathbf{P})=\gamma\sqrt{8E_AE_BE_C}&\sum_{M_{L_A},M_{S_A},M_{L_B},M_{S_B},M_{L_C},M_{S_C}}\langle L_AM_{L_A}S_AM_{S_A}|J_AM_{J_A}\rangle\langle L_BM_{L_B}S_BM_{S_B}|J_BM_{J_B}\rangle\\&\times\langle L_CM_{L_C}S_CM_{S_C}|J_CM_{J_C}\rangle\langle 1m1-m|00\rangle\langle\chi^{14}_{S_BM_{S_B}}\chi^{32}_{S_CM_{S_C}}|\chi^{12}_{S_AM_{S_A}}\chi^{34}_{1-m}\rangle\\&\times[\langle\phi^{14}_B\phi^{32}_C|\phi^{12}_A\phi^{34}_0\rangle\mathcal{I}(\mathbf{P},m_2,m_1,m_3)+(-1)^{1+S_A+S_B+S_C}\langle\phi^{32}_B\phi^{14}_C|\phi^{12}_A\phi^{34}_0\rangle\mathcal{I}(-\mathbf{P},m_2,m_1,m_3)],\end{aligned}\tag{B3}$$

where γ reflects the creation possibility of a quark pair $q_3\bar{q}_4$ from the vacuum, which is generally considered to be a universal constant for the decay of a specific meson system and can be determined by the relevant experimental data. It needs to be mentioned that the creation strength for the $s\bar{s}$ pair creation is different from that of the $u\bar{u}+d\bar{d}$ pair, where there exists the relation $\gamma_s=\gamma_u/\sqrt{3}$ [54]. Additionally, m_3 is the mass of constituent quark q_3, and ϕ_0 is the flavor wave function of $q_3\bar{q}_4$ pair. The expression of the momentum space integral $\mathcal{I}(\mathbf{P},m_2,m_1,m_3)$ reads as

$$\begin{aligned}\mathcal{I}(\mathbf{P},m_2,m_1,m_3)=&\int d^3\boldsymbol{p}\psi^*_{n_BL_BM_{L_B}}\left(\frac{m_3}{m_1+m_3}\mathbf{P}+\boldsymbol{p}\right)\\&\times\psi^*_{n_CL_CM_{L_C}}\left(\frac{m_3}{m_2+m_3}\mathbf{P}+\boldsymbol{p}\right)\\&\times\psi_{n_AL_AM_{L_A}}(\mathbf{P}+\boldsymbol{p})\mathcal{Y}^m_1(\boldsymbol{p}),\end{aligned}\tag{B4}$$

where $\mathcal{Y}^m_1(\boldsymbol{p})$ denotes the solid harmonic polynomial.

[1] M. Ablikim *et al.* (BESIII Collaboration), Measurement of $e^+e^-\to K^+K^-$ cross section at $\sqrt{s}=2.00$–3.08 GeV, Phys. Rev. D **99**, 032001 (2019).

[2] M. Ablikim *et al.* (BESIII Collaboration), Observation of a Resonant Structure in $e^+e^-\to K^+K^-\pi^0\pi^0$, Phys. Rev. Lett. **124**, 112001 (2020).

[3] P. A. Zyla *et al.* (Particle Data Group), Review of particle physics, Prog. Theor. Exp. Phys. **2020**, 083C01 (2020).

[4] B. Aubert *et al.* (*BABAR* Collaboration), A structure at 2175-MeV in $e^+e^-\to\phi f_0(980)$ observed via initial-state radiation, Phys. Rev. D **74**, 091103 (2006).

[5] C. P. Shen *et al.* (Belle Collaboration), Observation of the $\phi(1680)$ and the $Y(2175)$ in $e^+e^-\to\phi\pi^+\pi^-$, Phys. Rev. D **80**, 031101 (2009).

[6] M. Ablikim *et al.* (BES Collaboration), Observation of $Y(2175)$ in $J/\psi\to\eta\phi f_0(980)$, Phys. Rev. Lett. **100**, 102003 (2008).

[7] M. Ablikim *et al.* (BESIII Collaboration), Study of $J/\psi\to\eta\phi\pi^+\pi^-$ at BESIII, Phys. Rev. D **91**, 052017 (2015).

[8] G. J. Ding and M. L. Yan, A candidate for 1^{--} strangeonium hybrid, Phys. Lett. B **650**, 390 (2007).

[9] T. Barnes, N. Black, and P. R. Page, Strong decays of strange quarkonia, Phys. Rev. D **68**, 054014 (2003).

[10] C. Q. Pang, Excited states of ϕ meson, Phys. Rev. D **99**, 074015 (2019).

[11] X. Wang, Z. F. Sun, D. Y. Chen, X. Liu, and T. Matsuki, Non-strange partner of strangeonium-like state $Y(2175)$, Phys. Rev. D **85**, 074024 (2012).

[12] G. J. Ding and M. L. Yan, $Y(2175)$: Distinguish hybrid state from higher quarkonium, Phys. Lett. B **657**, 49 (2007).

[13] B. B. Malabarba, X. L. Ren, K. P. Khemchandani, and A. Martinez Torres, Partial decay widths of $\phi(2170)$ to kaonic resonances, Phys. Rev. D **103**, 016018 (2021).

[14] A. Martinez Torres, K. P. Khemchandani, L. S. Geng, M. Napsuciale, and E. Oset, The X(2175) as a resonant state of the phi K anti-K system, Phys. Rev. D **78**, 074031 (2008).

[15] F. E. Close and P. R. Page, The production and decay of hybrid mesons by flux tube breaking, Nucl. Phys. **B443**, 233 (1995).

[16] F. E. Close and S. Godfrey, Charmonium hybrid production in exclusive B meson decays, Phys. Lett. B **574**, 210 (2003).

[17] S. L. Zhu, Masses and decay widths of heavy hybrid mesons, Phys. Rev. D **60**, 014008 (1999).

[18] S. L. Zhu, Some decay modes of the 1^{-+} hybrid meson in QCD sum rules revisited, Phys. Rev. D **60**, 097502 (1999).

[19] J. P. Lees *et al.* (*BABAR* Collaboration), Precision measurement of the $e^+e^- \to K^+K^-(\gamma)$ cross section with the initial-state radiation method at BABAR, Phys. Rev. D **88**, 032013 (2013).

[20] B. Aubert *et al.* (*BABAR* Collaboration), Measurements of $e^+e^- \to K^+K^-\eta$, $K^+K^-\pi^0$ and $K^0_sK^\pm\pi^\mp$ cross-sections using initial state radiation events, Phys. Rev. D **77**, 092002 (2008).

[21] J. Z. Wang, D. Y. Chen, X. Liu, and T. Matsuki, Constructing J/ψ family with updated data of charmoniumlike Y states, Phys. Rev. D **99**, 114003 (2019).

[22] J. Z. Wang, R. Q. Qian, X. Liu, and T. Matsuki, Are the Y states around 4.6 GeV from e^+e^- annihilation higher charmonia?, Phys. Rev. D **101**, 034001 (2020).

[23] J. Z. Wang, Z. F. Sun, X. Liu, and T. Matsuki, Higher bottomonium zoo, Eur. Phys. J. C **78**, 915 (2018).

[24] C. Q. Pang, J. Z. Wang, X. Liu, and T. Matsuki, A systematic study of mass spectra and strong decay of strange mesons, Eur. Phys. J. C **77**, 861 (2017).

[25] Q. T. Song, D. Y. Chen, X. Liu, and T. Matsuki, Charmed-strange mesons revisited: Mass spectra and strong decays, Phys. Rev. D **91**, 054031 (2015).

[26] Q. T. Song, D. Y. Chen, X. Liu, and T. Matsuki, Higher radial and orbital excitations in the charmed meson family, Phys. Rev. D **92**, 074011 (2015).

[27] J. Z. Wang, D. Y. Chen, Q. T. Song, X. Liu, and T. Matsuki, Revealing the inner structure of the newly observed $D^*_2(3000)$, Phys. Rev. D **94**, 094044 (2016).

[28] L. S. Geng, E. Oset, L. Roca, and J. A. Oller, Clues for the existence of two $K_1(1270)$ resonances, Phys. Rev. D **75**, 014017 (2007).

[29] L. Roca, E. Oset, and J. Singh, Low lying axial-vector mesons as dynamically generated resonances, Phys. Rev. D **72**, 014002 (2005).

[30] X. Zhang, C. Hanhart, U. G. Meißner, and J. J. Xie, Remarks on non-perturbative three–body dynamics and its application to the $KK\bar{K}$ system, arXiv:2107.03168.

[31] I. Filikhin, R. Y. Kezerashvili, V. M. Suslov, S. M. Tsiklauri, and B. Vlahovic, Three-body model for $K(1460)$ resonance, Phys. Rev. D **102**, 094027 (2020).

[32] A. Martinez Torres, D. Jido, and Y. Kanada-En'yo, Theoretical study of the $KK\bar{K}$ system and dynamical generation of the $K(1460)$ resonance, Phys. Rev. C **83**, 065205 (2011).

[33] R. Y. Kezerashvili, S. M. Tsiklauri, and N. Z. Takibayev, Lightest kaonic nuclear clusters, arXiv:1510.00478.

[34] T. Bauer and D. R. Yennie, Corrections to VDM in the photoproduction of vector mesons. 1. Mass dependence of amplitudes, Phys. Lett. **60B**, 165 (1976).

[35] T. Bauer and D. R. Yennie, Corrections to diagonal VDM in the photoproduction of vector mesons. 2. Phi-omega mixing, Phys. Lett. **60B**, 169 (1976).

[36] D. Y. Chen, X. Liu, and T. Matsuki, Two charged strangeonium-like structures observable in the $Y(2175) \to \phi(1020)\pi^+\pi^-$ process, Eur. Phys. J. C **72**, 2008 (2012).

[37] Y. Huang, J. J. Xie, X. R. Chen, J. He, and H. F. Zhang, The $\gamma p \to na_2^+(1320) \to n\rho^0\pi^+$ reactions within an effective Lagrangian approach, Int. J. Mod. Phys. E **23**, 1460002 (2014).

[38] J. J. Xie, The $K^-p \to f_1(1285)\Lambda$ reaction within an effective Lagrangian approach, Phys. Rev. C **92**, 065203 (2015).

[39] D. Y. Chen, J. Liu, and J. He, Reconciling the $X(2240)$ with the $Y(2175)$, Phys. Rev. D **101**, 074045 (2020).

[40] S. Godfrey and N. Isgur, Mesons in a relativized quark model with chromodynamics, Phys. Rev. D **32**, 189 (1985).

[41] T. Barnes, F. E. Close, P. R. Page, and E. S. Swanson, Higher quarkonia, Phys. Rev. D **55**, 4157 (1997).

[42] D. P. Stanley and D. Robson, Nonperturbative potential model for light and heavy quark anti-quark systems, Phys. Rev. D **21**, 3180 (1980).

[43] D. Ebert, R. N. Faustov, and V. O. Galkin, Mass spectra and Regge trajectories of light mesons in the relativistic quark model, Phys. Rev. D **79**, 114029 (2009).

[44] D. Ebert, R. N. Faustov, and V. O. Galkin, Masses of light mesons in the relativistic quark model, Mod. Phys. Lett. A **20**, 1887 (2005).

[45] S. Ishida and K. Yamada, Light quark meson spectrum in the covariant oscillator quark model with one gluon exchange effects, Phys. Rev. D **35**, 265 (1987).

[46] A. V. Anisovich, C. A. Baker, C. J. Batty, D. V. Bugg, V. A. Nikonov, A. V. Sarantsev, V. V. Sarantsev, and B. S. Zou, Partial wave analysis of $\bar{p}p$ annihilation channels in flight with $I = 1$, $C = +1$, Phys. Lett. B **517**, 261 (2001).

[47] A. V. Anisovich, C. J. Batty, D. V. Bugg, V. A. Nikonov, and A. V. Sarantsev, A fresh look at $\eta_2(1645)$, $\eta_2(1870)$, $\eta_2(2030)$ and $f_2(1910)$ in $\bar{p}p \to \eta 3\pi^0$, Eur. Phys. J. C **71**, 1511 (2011).

[48] A. V. Anisovich, C. A. Baker, C. J. Batty, D. V. Bugg, L. Montanet, V. A. Nikonov, A. V. Sarantsev, V. V. Sarantsev, and B. S. Zou, Combined analysis of meson channels with $I = 1$, $C = -1$ from 1940 to 2410 MeV, Phys. Lett. B **542**, 8 (2002).

[49] D. V. Amelin *et al.* (VES Collaboration), Natural parity resonances in $\eta\pi^+\pi^-$, Nucl. Phys. **A668**, 83 (2000).

[50] B. Aubert *et al.* (*BABAR* Collaboration), The $e^+e^- \to 3(\pi^+\pi^-), 2(\pi^+\pi^-\pi^0)$ and $K^+K^-2(\pi^+\pi^-)$ cross sections at center-of-mass energies from production threshold to

4.5-GeV measured with initial-state radiation, Phys. Rev. D **73**, 052003 (2006).
[51] D. V. Bugg, Four sorts of meson, Phys. Rep. **397**, 257 (2004).
[52] L. M. Wang, J. Z. Wang, and X. Liu, Toward $e^+e^- \to \pi^+\pi^-$ annihilation inspired by higher ρ mesonic states around 2.2 GeV, Phys. Rev. D **102**, 034037 (2020).
[53] L. Micu, Decay rates of meson resonances in a quark model, Nucl. Phys. **B10**, 521 (1969).
[54] A. Le Yaouanc, L. Oliver, O. Pene, and J. C. Raynal, Why is $\psi(4.414)$ SO narrow?, Phys. Lett. **72B**, 57 (1977).
[55] M. Jacob and G. C. Wick, On the general theory of collisions for particles with spin, Ann. Phys. (N.Y.) **7**, 404 (1959); **281**, 774 (2000).